Organic passivation layer on flexible Surlyn substrate for encapsulating organic photovoltaics

Sindhu Seethamraju, Praveen C. Ramamurthy, and Giridhar Madras

Articles you may be interested in

Characterization of CZTSSe photovoltaic device with an atomic layer-deposited passivation layer
Appl. Phys. Lett. 105, 042108 (2014); 10.1063/1.4891852

Flexible field-effect transistor arrays with patterned solution-processed organic crystals
AIP Advances 3, 052123 (2013); 10.1063/1.4807669

Structural modifications of zinc phthalocyanine thin films for organic photovoltaic applications
J. Appl. Phys. 111, 103117 (2012); 10.1063/1.4721409

Tilted bulk heterojunction organic photovoltaic cells grown by oblique angle deposition
Appl. Phys. Lett. 95, 123309 (2009); 10.1063/1.3236838

Flexible organic photovoltaics using conducting polymer electrodes
Appl. Phys. Lett. 86, 093502 (2005); 10.1063/1.1867568

Organic passivation layer on flexible Surlyn substrate for encapsulating organic photovoltaics

Sindhu Seethamraju,[1] Praveen C. Ramamurthy,[1,2] and Giridhar Madras[3]
[1]Centre for Nanoscience and Engineering, Indian Institute of Science, Bangalore 560012, India
[2]Department of Materials Engineering, Indian Institute of Science, Bangalore 560012, India
[3]Department of Chemical Engineering, Indian Institute of Science, Bangalore 560012, India

Barrier materials are required for encapsulating organic devices. A simple methodology based on organic passivation layer on a flexible substrate has been developed in this work. Stearyl stearate (SS) was directly coated over the flexible Surlyn film. The barrier films with SS passivation layer exhibited much lower water vapor transmission rates compared to the neat Surlyn films. Moreover, the effect of the process of deposition of organic passivation layer on the resultant water vapor properties of the barrier films was evaluated. The accelerated lifetime studies conducted on encapsulated organic photovoltaics showed that the passivation layer improved the device performance by several fold compared to the non-passivated barrier films. © 2014 AIP Publishing LLC.
[http://dx.doi.org/10.1063/1.4895719]

The use of barrier materials spans a wide range of packaging industries such as food, pharmaceuticals, optics, and electronics. Ultra low water vapor and oxygen permeable, protective barrier coatings or passivation layers enable the commercialization of flexible organic electronic devices such as organic photovoltaics (OPVs), organic light emitting diodes (OLEDs), and organic field effect transistors (OFETs).[1–3] These devices require flexible, viable, thermally stable, and roll processable encapsulants with ultra high gas barrier.[4] Gases such as H_2O and O_2 are detrimental to organic devices due to the degradation of active components used in the devices and formation of dark spots.[5,6] The permeation of polar H_2O molecules further enhances the degradation activity due to oxygen and light.[7,8]

Though polymeric substrates offer flexible and an economic solution for encapsulating organic devices, they do not meet the requirement of ultra low water vapor transmission rates (WVTRs) of $<10^{-6}$ g m^{-2} day^{-1} and oxygen transmission rates (OTRs) of $<10^{-5}$ cc m^{-2} day^{-1}. Therefore, various inorganic passivation layers, such as Al_2O_3, SiO_2, SiC, TiO_2, and SiN_x, based on atomic layer deposition (ALD), physical vapor deposition (PVD), and plasma enhanced chemical vapor deposition (CVD) have been being developed to achieve ultra low WVTRs.[9–13] These single layered inorganic passivation layers deposited on flexible polymeric substrates, such as polyethylene terephthalate (PET) and poly ethylene naphthalate (PEN), offer permeation rates only up to $\sim10^{-2}$ g m^{-2} day^{-1}.[14,15] In the case of multiple, thicker and multilayered coatings (with 5–6 bilayers of inorganic/organic layers) much lower WVTR ($\sim10^{-5}$ g m^{-2} day^{-1}) have been achieved.[16–18] However, the presence of defect sites/pinholes on the passivation layers affects the resultant barrier properties.[19–21]

The defects and pinholes in the thin films are formed during their growth on polymer substrates due to the presence of dust particles, surface inhomogeneities on substrates, and generated stresses while deposition. Thus, defect sites are inevitable on such thin films coated on polymers. Therefore, few researchers have worked on the

deposition of organic molecules along with inorganic oxides to decrease the extent of formation of defective films.[22,23] However, this modification further complicates the process of deposition and requires to be optimized for the formation of defect free films. The presence of structural sub-nanometer defects and pinholes in the deposited layers affects the performance of the barrier and controls the residual WVTR and OTRs. Further, the detection of the defect sites at nano scale has been another challenging aspect.[21] The vacuum based processes, such as ALD and PVD, used for the deposition of these passivation layers are also complicated, expensive, and not suitable for roll processing. Therefore, much simpler and economically viable ultra low permeable barrier coatings need to be developed. Dense thin film hydrophobic coatings of organic molecules over flexible substrates could offer a better solution for achieving lower WVTRs.

The process of permeation through the polymer matrix occurs by dissolution of permeant and diffusion through the matrix. In the case of inorganic passivation layers, the permeation is through the defect sites or pinholes. When hydrophobic compounds are deposited on polymer substrates, lower WVTRs can be achieved due to the high energy barrier offered for the penetration of polar molecules such as H_2O. Further, the formation of pinholes and defect sites can be avoided in organic coatings. Therefore, in this letter, we show the ability of organic passivation layers on polymers in improving moisture barrier.

Octadecyl octadecanoate (Stearyl stearate, SS) was synthesized by esterification reaction from stearic acid and stearyl alcohol and used for fabricating the barrier material.[24] Stearic acid and stearyl alcohol are taken in 1:1 molar ratio along with the catalyst, $SnCl_2$ (10 mmol/mol) into a round bottomed flask. The reaction was carried under inert conditions at 85 °C for 24 h. The formation of SS was verified by Fourier transformed infra red spectroscopy (FTIR) spectroscopy. The melting temperatures for SS and neat Surlyn were found to be at ~59 °C and 98 °C, respectively, from

differential scanning calorimetry (DSC), shown in Figure S1 in the supplementary material.[25]

The barrier films were fabricated by following three different methodologies. The first set of samples was prepared by spin coating of dissolved SS in hexane, at 1500 rpm over the Surlyn film. The second set of samples was fabricated by direct spin coating (4000 rpm) of melted SS at 80 °C. The Surlyn substrate was maintained at 100 °C during spin coating. Third set of samples was obtained by organic thermal evaporation of SS on to Surlyn at ∼10 Å s⁻¹ at ∼ 275 °C. The Surlyn substrate was maintained at 75 °C during the deposition in order to improve the adhesion of SS. The samples were designated as SSC, MSC, and OTE for solvent spin coating, melt spin coating, and organic thermal evaporation, respectively. SS was coated in three weight percentages, 5%, 10%, and 15%, for each method of deposition and numbered as 1, 2, and 3, respectively. Deposition of higher weight content resulted in flaking of SS due to poor adhesion and, therefore, was not studied further. Neat Surlyn film was designated as S0.

The depression in melting point of Surlyn was observed with increasing the weight content of SS from 5% to 15% over Surlyn film from DSC (Figure S1). The melting point decreased by 9 °C for S0 to MSC1 and a further 9 °C from MSC1 to MSC2. This reduction in melting point is due to the reduction in enthalpic contributions to the melting of Surlyn with the addition of SS resulting from the positive interactions between the two components.

The WVTRs through the barrier films were measured using the Ca-test method. In Ca-test, the degradation of calcium thin film due to oxidation of metallic calcium is determined from the increase of resistance with time due to the formation of nonmetallic $Ca(OH)_2$.[26] It is further correlated with the number of H_2O molecules permeating through the barrier film used for sealing the calcium thin film to calculate WVTR using the following equation:

$$WVTR = -2\frac{MH_2O}{MCa}\partial\rho\left(\frac{l}{b}\right)\frac{d\left(\frac{1}{R}\right)}{dt}. \quad (1)$$

Calcium thin films of 200 μm thick (1 × 1 cm²) were thermally evaporated on to cleaned glass substrates at the centre. Aluminium electrodes were deposited on either side to take electrical contacts for resistance measurements (schematic shown in Figure S2).[25,27] These devices were further sealed with neat Surlyn and SS coated barrier films, using epoxy sealant on the edges. Thus, sealed calcium devices were exposed to humid environment at ∼95% RH and 35 °C. The calcium thin film resistances were monitored with time (Figures 1(a)–1(c)) and the WVTRs through the barrier films were calculated using Eq. (1) and given in Figures S3(a)–S3(c).[25]

The WVTR through the neat Surlyn film was observed to be ∼4 g m⁻² day⁻¹. The barrier films with spin coated SS by dissolving in solvent exhibited one order reduction in WVTR with ∼0.18, 0.14, and 0.015 g m⁻² day⁻¹ for SSC1, SSC2, and SSC3 films, respectively (Figure 1(a)). The samples with melt spin coated SS exhibited lower values of ∼0.08, 0.06, and 0.01 g m⁻² day⁻¹ for MSC1, MSC2, and
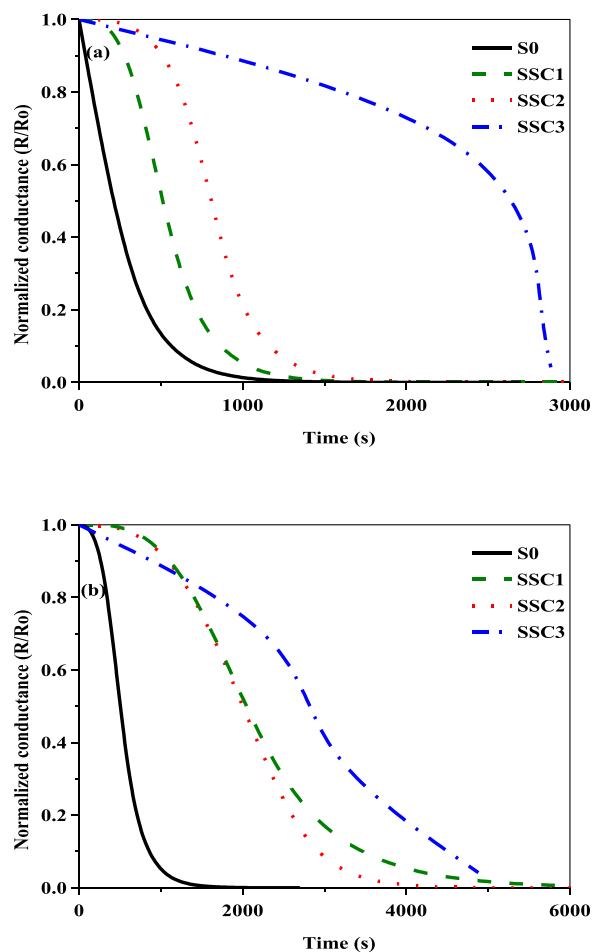

FIG. 1. Reduction in normalized conductance from calcium degradation test for the films by (a) solvent spin coating, (b) melt spin coating, and (c) thermal evaporation of SS.

MSC3 films, respectively, with ∼2 order decrease in water vapor permeabilities (Figure 1(b)). The films with thermally evaporated SS, OTE1, OTE2, and OTE3 exhibited lowest values for WVTR ∼0.006, 0.001, and 0.0001 g m⁻² day⁻¹, respectively (Figure 1(c)). This shows that the simple coating of SS by organic thermal evaporation over Surlyn decreased the water vapor permeation by ∼4 orders. These results show that the thermally evaporated SS showed better performance for moisture barrier compared to spin coated SS. With increasing the weight content of SS over Surlyn, the WVTRs decreased for all the processes of deposition, resulting in lower values for samples with 15 wt. % of SS.

Water contact angle measurements were carried out to determine the effect of coating on the hydrophobicity of the neat Surlyn film. It can be observed that the hydrophobicity of the Surlyn film increased from 78° to 105° (±5°) for passivated Surlyn films due to the coating of SS (Figure S4).[25] The contact angle did not vary significantly for different processes of deposition of SS. This shows that the SS coating increased the hydrophobicity of the Surlyn films.

To investigate the effect of organic thin film passivation layer of SS on organic devices, OPVs were fabricated, encapsulated with S0, SSC3, MSC3, and OTE3 films as shown in the schematic Figure S5.[25] These were subjected to accelerated weathering studies (at ∼65 °C and 95% RH). The lifetimes of the devices under these accelerated conditions are
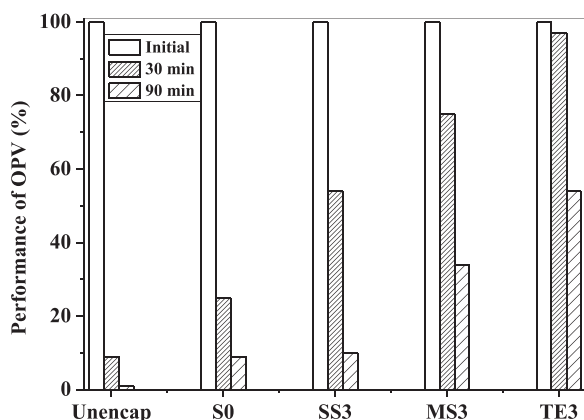
FIG. 2. Accelerated aging studies for encapsulated devices with neat Surlyn and SS coated Surlyn barrier films.

equivalent to ∼1000 times the lifetimes at 25 °C and 45% RH.[28,29] Representative I-V curves for the encapsulated (S0, SSC3, MSC3, and OTE3) and unencapsulated devices are given in Figure S6.[25] From device (I-V) characteristics, it was observed that the device current decreases with increasing time of exposure to accelerate weathering conditions. This can be attributed to the increased moisture content in the device, which causes change of active layer morphologies in the device.[8]

The average decrease in the normalized OPV efficiencies for at least 3 encapsulated devices is used to evaluate the performance of the barrier films used for encapsulation (Figure 2). The performance of the unencapsulated device dropped to ∼1% in 30 min. This shows that the OPV devices are unstable in humid environment. The OPV devices encapsulated with the Surlyn films deposited with thermally evaporated SS (OTE3) retained ∼97%, while the device encapsulated with neat Surlyn could retain only 10% of its initial performance after 30 min of accelerated aging (Figure 2). The Surlyn films with spin coated SS by melting and solution could retain ∼75% (MSC3) and 55% (SSC3) of their initial performances, respectively. After 90 min of accelerated weathering, the encapsulated OPV devices by thermal evaporation, melt and spin coatings, exhibited 54%, 34%, and 11% of their initial performances, respectively. This shows that the barrier films with the SS passivation layers are effective in protecting the devices from moisture.

In layered coatings of inorganic oxides such as silica and alumina, the WVTRs do not change with time.[14,15,17] However, the diffusion of gases through these organic coatings varies with time. The gases permeate through the free volume between the organic molecules and generate a continuous pathway over a time period. Therefore, water vapor permeation increases with time. At longer time periods, permeation pathways form through the organic barrier layers resulting in higher water vapor permeabilities when compared to initial values. Moreover, with increasing time of aging, water molecules accumulating in the encapsulated device increases. The morphology of active layers in the device changes due to the diffusion of H_2O molecules and degradation of active components resulting in the decrease of device current. Therefore, after 90 min of accelerated aging, the device performance decreased significantly. The devices encapsulated with OTE3

showed the best performances among all the encapsulated OPV devices for water vapor barrier followed by MSC3 and SSC3 films, which is in agreement with the previously discussed WVTR results.

Three different processes, namely, SSC, MSC, and OTE were used for the fabrication of SS coating on Surlyn. It can be clearly observed that the resulting barrier properties are dependent on the process of deposition and are influenced by molecular orientation and arrangement. In the case of SSC, solvent was used and in MSC, the melt SS was directly employed. The volatile solvent evaporates leading to the formation of porous film resulting in lower water vapor barrier when compared to that observed in MSC samples. In thermal evaporation, SS sublimes and deposits on the substrate resulting in an ordered assembly compared to that obtained by spin coating. Further, thermal evaporation is conducted in vacuum ($<4 \times 10^{-6}$ bars) compared to spin coating process, which is carried out under atmospheric condition. Therefore, the SS layer on Surlyn is more uniform and ordered in OTE samples compared to the samples prepared by spin coating. Thus, OTE samples exhibited the highest barrier to water vapor.

In conclusion, three approaches have been employed in this work with simple and viable processing to design better water vapor barrier materials. SS has been coated on to flexible Surlyn film by spin coating and thermal evaporation to improve the water vapor barrier. The increase of water contact angles suggests the hydrophobic nature of SS. The WVTR decreased by four orders for thermally evaporated SS over Surlyn film. Moreover, the prolonged performances (under accelerated weather conditions) of the encapsulated OPV devices with SS on Surlyn when compared to neat Surlyn indicate the effectiveness of the organic passivation layer on flexible polymer substrates.

[1]M. Jørgensen, K. Norrman, and F. C. Krebs, Sol. Energy Mater. Sol. Cells **92**, 686 (2008).

[2]C. J. Brabec, J. A. Hauch, P. Schilinsky, and C. Waldauf, MRS Bull. **30**, 50 (2005).

[3]H. Jeon, K. Shin, C. Yang, C. E. Park, and S.-H. K. Park, Appl. Phys. Lett. **93**, 163304 (2008).

[4]M. Pagliaro, R. Ciriminna, and G. Palmisano, ChemSusChem **1**, 880 (2008).

[5]P. E. Burrows, V. Bulovic, S. R. Forrest, L. S. Sapochak, D. M. McCarty, and M. E. Thompson, Appl. Phys. Lett. **65**, 2922 (1994).

[6]K. Norrman, S. A. Gevorgyan, and F. C. Krebs, ACS Appl. Mater. Interfaces **1**, 102 (2009).

[7]J. A. Hauch, P. Schilinsky, S. A. Choulis, S. Rajoelson, and C. J. Brabec, Appl. Phys. Lett. **93**, 103306 (2008).

[8]H. Hintz, H.-J. Egelhaaf, L. Lüer, J. Hauch, H. Peisert, and T. Chassé, Chem. Mater. **23**, 145 (2011).

[9]G. Dennler, C. Lungenschmied, H. Neugebauer, N. S. Sariciftci, M. Latrèche, G. Czeremuszkin, and M. R. Wertheimer, Thin Solid Films **511–512**, 349 (2006).

[10]A. A. Dameron, S. D. Davidson, B. B. Burton, P. F. Carcia, R. S. McLean, and S. M. George, J. Phys. Chem. C **112**, 4573 (2008).

[11]W. Huang, X. Wang, M. Sheng, L. Xu, F. Stubhan, L. Luo, T. Feng, X. Wang, F. Zhang, and S. Zou, Mater. Sci. Eng., B **98**, 248 (2003).

[12]M. Schaepkens, T. W. Kim, A. G. Erlat, M. Yan, K. W. Flanagan, C. M. Heller, and P. A. McConnelee, J. Vac. Sci. Technol., A **22**, 1716 (2004).

[13]A. B. Chwang, M. A. Rothman, S. Y. Mao, R. H. Hewitt, X. Chu, L. Moro, T. Trajewski, and N. Rutherford, Appl. Phys. Lett. **83**, 413 (2003).

[14]P. F. Carcia, R. S. McLean, M. H. Reilly, M. D. Groner, and S. M. George, Appl. Phys. Lett. **89**, 031915 (2006).

[15]E. Langereis, M. Creatore, S. B. S. Heil, M. C. M. van de Sanden, and W. M. M. Kessels, Appl. Phys. Lett. **89**, 081915 (2006).

[16]S. W. Seo, E. Jung, S. Joon Seo, H. Chae, H. Kyoon Chung, and S. Min Cho, J. Appl. Phys. **114**, 143505 (2013).

[17]J. Granstrom, M. Villet, T. Chatterjee, J. A. Gerbec, E. Jerkunica, and A. Roy, Appl. Phys. Lett. **95**, 093306 (2009).

[18]J. Meyer, H. Schmidt, W. Kowalsky, T. Riedl, and A. Kahn, Appl. Phys. Lett. **96**, 243308 (2010).

[19]A. S. da Silva Sobrinho, G. Czeremuszkin, M. Latrèche, and M. R. Wertheimer, J. Vac. Sci. Technol. A **18**, 149 (2000).

[20]A. S. da Silva Sobrinho, G. Czeremuszkin, M. Latreche, and M. R. Wertheimer, Appl. Phys. A: Mater. Sci. Process. **68**, 103 (1999).

[21]A. S. da Silva Sobrinho, G. Czeremuszkin, M. Latreche, G. Dennler, and M. R. Wertheimer, Surf. Coat. Technol. **116–119**, 1204 (1999).

[22]N. Kim, W. J. Potscavage, B. Domercq, B. Kippelen, and S. Graham, Appl. Phys. Lett. **94**, 163308 (2009).

[23]W. Cho, K. Sung, K.-S. An, S. Sook Lee, T.-M. Chung, and Y. Kim, J. Vac. Sci. Technol., A **21**, 1366 (2003).

[24]J. Otera and J. Nishikido, *Esterification: Methods, Reactions, and Applications* (Wiley, 2009).

[25]See supplementary material http://dx.doi.org/10.1063/1.4895719 for schematics and figures..

[26]R. Paetzold, A. Winnacker, D. Henseler, V. Cesari, and K. Heuser, Rev. Sci. Instrum. **74**, 5147 (2003).

[27]S. Seethamraju, P. C. Ramamurthy, and G. Madras, ACS Appl. Mater. Interf. **5**, 4409 (2013).

[28]S. Gupta, S. Sindhu, K. A. Varman, P. C. Ramamurthy, and G. Madras, RSC Adv. **2**, 11536 (2012).

[29]M. O. Reese, S. A. Gevorgyan, M. Jørgensen, E. Bundgaard, S. R. Kurtz, D. S. Ginley, D. C. Olson, M. T. Lloyd, P. Morvillo, E. A. Katz, A. Elschner, O. Haillant, T. R. Currier, V. Shrotriya, M. Hermenau, M. Riede, K. R. Kirov, G. Trimmel, T. Rath, O. Inganäs, F. Zhang, M. Andersson, K. Tvingstedt, M. Lira-Cantu, D. Laird, C. McGuiness, S. (Jimmy) Gowrisanker, M. Pannone, M. Xiao, J. Hauch, R. Steim, D. M. DeLongchamp, R. Rösch, H. Hoppe, N. Espinosa, A. Urbina, G. Yaman-Uzunoglu, J.-B. Bonekamp, A. J. J. M. van Breemen, C. Girotto, E. Voroshazi, and F. C. Krebs, Sol. Energy Mater. Sol. Cells **95**, 1253 (2011).